



Published in final edited form as:

Hum Mov Sci. 2009 April ; 28(2): 169–190. doi:10.1016/j.humov.2009.01.003.

DOES HAND DOMINANCE AFFECT THE USE OF MOTOR ABUNDANCE WHEN REACHING TO UNCERTAIN TARGETS?

Sandra Maria Sbeghen Ferreira Freitas and John Peter Scholz

Department of Physical Therapy, University of Delaware, Newark, USA

Abstract

This study investigated hemispheric differences in utilizing motor abundance to achieve flexible patterns of joint coordination when reaching to uncertain target locations. Right-handed participants reached with each arm to the same central target when its final location was certain or when there was a 66% probability that its location could change after movement initiation. Use of greater motor abundance was observed when participants reached to the central target under target location uncertainty regardless of the arm used to reach. Joint variance associated with variability of movement direction was larger when reaching with the left, non-dominant arm. This arm also exhibited higher hand path variability compared to the dominant arm. These arm differences were not found when then final (central) target location was known in advance. The results provide preliminary evidence for a greater ability of the dominant (right) arm/left hemisphere to decouple directions in joint space. That is, to increase the use of motor abundance without simultaneously inducing unwanted hand path variability requires that joint variations be restricted to a limited subspace of joint space. Hemispheric differences in motor planning did not appear to account for arm differences related to the use of motor abundance.

Keywords

hand dominance; arm-reaching movements; uncontrolled manifold; double-step paradigm; motor abundance; motor planning

1. Introduction

Multiple combinations of arm joint movements can be used to reach the same spatial target because of motor redundancy (Bernstein, 1967), or when viewed more positively, motor abundance (Gelfand & Latash, 1998). Several studies have reported that the central nervous system (CNS) takes advantage of motor abundance when performing reaching tasks (Reisman & Scholz, 2003; Scholz, Schöner, & Latash, 2000; Tseng & Scholz, 2005; Tseng, Scholz, & Schöner, 2002). The assumption underlying these studies is that the CNS plans movements in terms of task-related parameters (i.e., control of reach direction or hand path extent), the plan being implemented by selecting functions that relate a family of joint angles or muscle contraction states to the desired values of the task parameters (Latash, Scholz, & Schöner, 2007; Scholz & Schöner, 1999; Schöner, 1995). This strategy allows for the flexible control

Address for correspondence: Dr. John P. Scholz, Department of Physical Therapy, Biomechanics and Movement Science Program, 307 McKinly Laboratory, University of Delaware, Newark, DE 19716, Office: 302-831-8666, FAX: 302-831-4234, jpscholz@udel.edu.

Publisher's Disclaimer: This is a PDF file of an unedited manuscript that has been accepted for publication. As a service to our customers we are providing this early version of the manuscript. The manuscript will undergo copyediting, typesetting, and review of the resulting proof before it is published in its final citable form. Please note that during the production process errors may be discovered which could affect the content, and all legal disclaimers that apply to the journal pertain.

of joint motions to achieve the appropriate values of the task parameters. This may be important for error compensation such as when reaching toward an uncertain target location (Freitas, Scholz, & Stehman, 2007).

1.1. Movement uncertainty and motor abundance

The double-step paradigm, where a target is shifted to a new location at movement onset, has been used in several studies investigating the effect of target uncertainty on the planning and control of arm movements (Georgopoulos, Kalaska, & Massey, 1981; Komilis, Péllisson, & Prablanc, 1993; Péllisson, Prablanc, Goodale, & Jeannerod, 1986; Prablanc & Martin, 1992; Robertson & Miall, 1997; Soechting & Lacquaniti, 1983). However, only few studies have investigated how uncertainty of the final target location during movement planning affects coordination. Soechting and Lacquaniti (1983) observed that target uncertainty resulted in greater inter-trial hand trajectory variability. In addition, the authors suggested that success at correcting the movement trajectory occurred by using stereotyped patterns of coupling among the arm muscles that resulted in a consistent linear relationship between the angular velocities of the shoulder and elbow joints. These characteristics of the movements were argued to simplify movement control by reducing the number of degrees of freedom (DOFs) that required independent control by the CNS.

In contrast, Robertson and Miall (1997) compared reaching under conditions of target uncertainty when the arm had three redundant joints and when redundancy was eliminated by preventing wrist movement during planar reaches, which then involved only shoulder and elbow motion. Greater path lengths were used to correct the movement trajectories toward a target shifted unexpectedly when movements were constrained to two joints. Based on these results, Robertson and Miall (1997) suggested that the CNS normally exploits the intrinsic redundancy of the limb to effectively control movements during an unpredictable perturbation of the target location. This study analyzed differences in reaching movements to new, but different target locations after a target had jumped from its initial location following movement initiation. Thus, it is not clear if the suggested use of motor abundance was related to movement to the new spatial location, to the uncertainty of target position, or both.

We investigated in a recent study the use of motor abundance when participants reached with their dominant right arm to an identical target location either when there was some probability that the target location could change after movement onset (uncertain condition) or when the target location remained fixed (Freitas et al., 2007). Motor abundance was characterized using the Uncontrolled Manifold (UCM) approach, which partitions the variance of elemental variables into a component reflecting the use of motor abundance to stabilize a task-relevant parameter and a component of variance leading to variability of the task-relevant parameter (Scholz & Schöner, 1999; Schöner, 1995). In that study, greater joint variance reflecting the use of motor abundance was found in the uncertain condition during both the acceleration and deceleration phases of movement, while there was no increase in the variance component affecting the stability of the hand's position. Thus, our findings were consistent with the conclusions of Robertson and Miall (1997). The results also suggest that the amount of motor abundance used when performing a task can be modified by motor planning which would provide an advantage when more flexibility is required. Whether the ability to take advantage of the flexibility provided by motor abundance differs between the hemispheres is, however, unknown and is the focus of this report.

1.2. Affects of hemispheric dominance on motor planning

Differences in movement planning related to arm dominance have been reported previously (Barthelemy & Boulinguez, 2001; Boulinguez, Barthelemy, & Debu, 2000; Boulinguez, Nougier, & Velay, 2001; Carson, Chua, Goodman, Byblow, & Elliott, 1995; Elliot & Chua,

1996; Elliott, Lyons, Chua, Goodman, & Carson, 1995; Hodges, Lyons, Cockell, Reed, & Elliott, 1997), although not related to movement coordination. Overall, these studies suggest that the dominant, left hemisphere has an advantage for movement execution whereas the non-dominant, right hemisphere may be superior for movement planning based on differences in reaction time between the right and left arms. An advantage of the right arm in movement execution was suggested to be related to the ability to precisely and rapidly reorganize the movements when a perturbation was applied to a target location (Elliott et al., 1995).

In contrast, results of studies of stroke survivors performing reaching movements with their non-paretic limbs suggested that the dominant, left hemisphere is superior at movement planning given observed deficits in the ballistic component of movement when that hemisphere was damaged (Winstein & Pohl, 1995). Individuals with a right stroke were shown to have deficits in processing visual information during more complex tasks, suggesting that the right hemisphere is better at rapid, on-line corrections that are more dependent on feedback (closed-loop).

The study reported here examined further the issue of hemispheric differences in planning and execution by investigating how target uncertainty affects the use of motor abundance by the dominant and non-dominant arms. We assumed that any arm differences observed during the acceleration phase of the movement were more likely due to differences in movement planning and are less dependent on sensory feedback than were differences observed after peak movement velocity (Haaland, Harrington, & Grice, 1993; Haaland, Prestopnik, Knight, & Lee, 2004; Marteniuk, MacKenzie, Jeannerod, Athènes, & Dugas, 1987; Winstein & Pohl, 1995). Differences during the deceleration phase, which includes final movement corrections, were assumed to be more dependent on feedback processes (Elliott, Binsted, & Heath, 1999; Soechting, 1984; Woodworth, 1899). If the use of motor abundance is affected by motor planning, as suggested by our recent findings (Freitas et al., 2007), and the hemispheres differ in the role they play in motor planning, then we expected differences in the use of motor abundance between the arms when reaching to the same target under an uncertain target condition but not under certain target conditions. Similarly, previously described hemispheric differences related to final arm adjustments should be evident during the deceleration phase of the task.

2. Methods

2.1. Participants

Eleven right hand dominant, healthy adults (five males and six females, mean age \pm SD: 26.5 \pm 10.5 yrs) participated in the reported study. Five participants performed the task first with their dominant right arm while six participants performed first with their non-dominant left arm. Hand dominance was determined by the Edinburgh handedness questionnaire (Oldfield, 1971). All participants gave informed consent as approved by the University's Human Subjects Review Board.

2.2. Apparatus and Data Acquisition

The three-dimensional (3D) kinematics of the arm and scapula were recorded at 120 Hz using a six-camera VICON motion measurement system. Rigid bodies with 4 markers each were placed on hand, lower arm, upper arm, and on the superior aspect of the upper trunk, two-thirds of the distance between the neck and the acromion process to capture clavicle/scapula motion. Individual markers were placed below the notch of the sternum and on the pointer-tip. The former marker served as the basis of the coordinate system. One static arm calibration trial was recorded prior to the experiment. Additional markers recorded during this trial were placed on the radial and ulnar styloid processes of the wrist and on the epicondyles of the elbow, the

mean position of which were used to estimate the joints' centers. Another marker lateral and just inferior to the acromion process was used to estimate the shoulder joint location. In this trial, the arm was facing forward from the shoulder, with the upper arm, forearm, and hand aligned and held parallel to the floor, the thumb pointing upward. In this position, the arm was parallel to the global y-axis and all joint angles were defined as zero. The X-axis of each joint pointed laterally, the Y-axis pointed along the long axis of the upper arm, forearm and hand, and the Z-axis pointed upward.

2.3. Experimental Procedure

Fig. 1a provides a schematic of the experimental set-up (right arm view). Participants were seated in an adjustable-height chair to ensure that their forearm rested on the table in pronation, with the upper arm nearly vertical and the elbow flexed to approximately 90°. Trunk motion was restrained by strapping it to the chair such that scapular motion was not restricted. Participants began each trial from the same initial position. To ensure that this position was consistent across trials and conditions, a bag full of foam beans was fitted around the lateral and medial aspect of the participants' arm. Then the air was extracted from the bag, leaving the arm in a trough with rigid sides. From this position, participants were instructed to reach and point to a target displayed on the computer monitor. A transparent touch-screen (Magic Touch, Keytec, Inc.) was placed over the video monitor to record the contact location of a pointer that was attached to a molded splint worn by the participant. The pointer-tip was set at a distance equal to the index finger's length when it was extended. The touch screen was set at a distance of approximately 95% of the measured distance from the acromion process of the shoulder to the tip of the index finger of the arm used to reach. A green 1.5-cm diameter circular target was displayed on the video monitor at the beginning of all trials, centered on the participant's midline.

Each participant performed approximately 160 trials of reaching with each arm. For all trials, participants were instructed to reach "as fast and as accurately as possible" to a target displayed at the center of the video monitor, at 70% of the participant's eye height. During the first block of 40 trials ("single-step trials"), the target location remained fixed throughout the trials (central target, CCT; Fig. 1b). The remaining 120 trials employed the "double-step" paradigm to create target location uncertainty (U). A target was always displayed initially at the central location, as for CCT trials. When the participants' hand moved from the initial position, a switch was released that could either have no effect on the central target location (UCT; 40 trials) or could result in the target jumping by 13-cm ipsilaterally (UIP; 40 trials) or contralaterally (UCL; 40 trials) to the participating arm, which corresponds to a 16.5° deviation of the vector pointing from the initial position to the center of the central target (Fig. 1c). Targets jumped approximately 16-ms after movement initiation and the target location was randomized across trials using a customized LabView™ program (National Instruments). For this block of trials, participants were instructed to adjust their reach to the new target if it jumped suddenly from the center location. A summary of the experimental design is presented in Table 1. Single-step (CCT) trials were performed before the double-step trials to prevent biasing the performance of the CCT trials by previously occurring random target "jumps". A ten-minute break was allowed between the block of CCT trials and the double-step trials. Before the beginning of each condition, participants practiced less than 10 trials for each condition to familiarize them with the task. Fatigue was never reported by the participants.

At the beginning of all trials, participants were told to fix their eyes on the centrally located target and start the movement as soon as they felt ready following an auditory signal. There was no reaction time requirement. The instruction during double-step trials was to initiate one smooth movement toward the central target, at the same movement speed as for the single-step trials. Then, if the target jumped, they were told to adjust their reach trajectory toward the new

target location. Participants were asked to not anticipate whether the target would jump or remain centered. Data were recorded for 3 s.

2.4. Data Analysis

Data analyses were performed using Matlab™ routines (Mathworks, Version 7.0). Kinematic data were low-pass filtered at 5 Hz using a bi-directional, second-order Butterworth filter before further processing. The marker data during dynamic trials were referenced back to the arm calibration trial to compute the 10 rotational DOFs of the arm: 3 DOFs each at the clavicle/scapula and shoulder joints and 2 DOFs each at the elbow and wrist joints. Joint angles were calculated using the algorithm proposed by Söderkvist and Wedin (1993). Joint angular velocities were calculated as the first derivatives of the joint angles' time-series.

The coordinates of the center target and the initial hand position were used to form a local coordinate system into which all marker data were rotated for further analyses. The x-axis of this local coordinate system was aligned with a vector from the hand's starting position to the target's center (corresponding to movement extent), and the y- and z-axes were formed orthogonal to this vector, following the right-hand rule (corresponding to two components of movement direction).

Movement onsets and terminations were defined, respectively, using 3% and 5% of the peak pointer-tip velocity. *Pointer-tip velocity* was obtained by computing the norm of the first derivatives of each coordinate of the pointer-tip position. A larger cutoff for movement termination was used to eliminate small final corrections used to stabilize the pointer-tip contact with the touch-screen. Determination of the time of maximum acceleration and deceleration (ACC_{PK} and DEC_{PK} , respectively) and the time of peak velocity (VEL_{PK}) of the pointer was done automatically and visually checked for accuracy later. Although the procedure to compute movement onsets and terminations can potentially affect the amount of movement variability, we do not believe that this is an issue in the current study for several reasons. First, the primary analysis (see Section 2.4.2) was performed for the movements to the central target under the certain (single-step) and uncertain (double-step) conditions only. As reported below, trials of reaching with neither arm nor condition differed in the magnitude of peak velocity or movement time. Therefore, the selection of movement onsets and terminations based on the percentages of peak velocity were consistent across conditions and arms. Second, we have performed previously an extensive test of the effect on partitioning of joint variance results of using different criteria for selecting movement onsets and terminations based on peak velocity and peak accelerations (unpublished data). Although different criteria lead to quantitative differences in the amount of variance, the relative magnitudes of the two components of variance (see below) were not affected qualitatively by those different criteria. Finally, although curve-fitting procedures can be used to determine movement onsets and terminations, which might have greater reliability, these procedures themselves are not foolproof (see (Liebermann, Biess, Gielen, & Flash, 2006)).

2.4.1. Dependent Variables—The following variables were used to describe the temporal characteristics of the participants' performance. *Movement onset time* (MOT) was defined as the time elapsed from the auditory signal, indicating to the participants that they could begin to reach at any time, until they actually initiated the reach. Although similar to reaction time, MOT differs in that participants were told to initiate their reaches only when they were ready to do so after the auditory signal. *Movement time* was defined as the time from movement onset until movement termination. The time to change movement direction, called *turning direction*, for the UIP and UCL conditions was calculated based on the method used by Soechting and Lacquaniti (1983). In this study, the velocity profile corresponding to movement direction was normalized with respect to the peak velocity of movement extent (local x-axis)

for both single-step (CCT) and double-step (UIP and UCL) trials. Then, for single-step trials, the average and standard deviation of the normalized velocity profile of movement direction was calculated. For double-step trials, the turning direction was defined as the time at which the normalized velocity profile of movement direction exceeded two standard deviations from the velocity profile for single-step trials.

To assess how accurately the participants performed the movements, we computed the *3D constant* and *variable errors* of pointing at movement termination, which was defined as the time when the pointer-tip reached 5% of peak velocity. *Linearity index* was defined as the ratio between the sum of the 3D linear distances between adjacent data points along the pointer-tip's movement path (the path length) and the length in 3D of a straight-line from the initial hand position to the center of the target. Hand trajectories with perfectly straight paths to the target should have a linearity index equal 1, whereas more curved hand trajectories should have a linearity index greater than 1. In addition, the spatial position of the pointer-tip (*x*-, *y*-axis) at the time of ACC_{PK} , VEL_{PK} , and DEC_{PK} were determined for each trial and used to calculate the pointer-tip directional deviation. *Directional deviation* was defined as the angle between (1) the vector pointing from the starting pointer-tip location to the pointer-tip's location at each event time (time of ACC_{PK} , VEL_{PK} , and DEC_{PK}), and (2) the vector pointing from the starting pointer-tip location to the center of the central target. Positive values were attributed to movements to the right of the straight line and negative values to the left of the straight line. Cumulative histogram (bin width = 1°) of the distribution of movement directions for all movements and across all participants and trials were plotted for each condition. Straight-line movements should have zero distribution around zero while trials with target jumps should be distributed around $\pm 16.5^\circ$. The data for double-step trials were fitted with normal distribution functions.

The total *variability of pointer-tip position* occurring orthogonal to a straight-line path to the target, i.e., movement direction, was computed from the pointer-tip marker at each time point across trials. Before this computation, each trial was time-normalized to 100 frames. Pointer-tip variability data were averaged within the acceleration phase (movement onset until the time of VEL_{PK}) and the deceleration phase (VEL_{PK} until the time of movement termination).

2.4.2. Uncontrolled Manifold (UCM) Approach—Motor abundance was computed using the UCM approach (Scholz & Schöner, 1999; Schöner, 1995). This approach uses geometric models that describe how changes in joint angles, or other motor elements, affect the value of specified task variables, such as the hand's position, to partition the variance of the joint configuration across repetitions into two components. One component is the variance of joint configurations that does not change the value of a relevant task variable and, therefore, indicates the use of motor abundance (variance component within UCM, null subspace, V_{UCM}). The other variance component is joint configuration variance that leads to unstable values of the task variable across repetitions (variance component orthogonal to UCM, range subspace, V_{ORT}).

For the current analysis, the joint configuration variance was that of the 10 joint motions (θ) and the task variable of interest was the direction of the pointer-tip's movement (r) with respect to a straight line to the target from the initial position. In the framework of the present experiments, control of the pointer-tip's movement direction should be reflected by the stability of this variable (i.e., low variability). In the space of the joints, this is reflected by low values of the variance component V_{ORT} . Equal stabilization of the pointer-tip's movement direction in the certain and uncertain conditions would be reflected by no differences in V_{ORT} across conditions. What about the other variance component, V_{UCM} ? By definition, it has no effect on the value of the task variable so that it can be, in principle, of any magnitude. However, if motor abundance provides for greater flexibility and if its level can be influenced by motor

planning, then one could predict higher values of V_{UCM} in the uncertain task condition, as was shown in our previous work (Freitas et al., 2007). Similarly, if the left hemisphere of right-handed individuals is more important for motor planning, then higher V_{UCM} can be expected when participants perform the uncertain targeting conditions with their dominant, right arm.

Note that a strict comparison of these measures across certain and uncertain (random) conditions was possible only for reaches toward the center target. Otherwise, once the hand trajectory begins to deviate substantially, different limb geometries across conditions makes conclusions about variance differences difficult (e.g., during the deceleration phase of the reach comparing UIP and UCL trials).

The following formal steps were carried out to perform the UCM analysis to investigate the above hypotheses. In the first step, the geometric model relating the pointer-tip position (\underline{r}) to the configuration of the 10 joint angles was determined as:

Pointer-tip position (r) = $R_{\theta_1} \times R_{\theta_{i+1}} \times \dots \times R_{\theta_n} (d_i + sl_h) + p_i + R_{\theta_i} \times p_{i+1} + \dots + R_{\theta_{n-1}} \times p_n$, where R_{θ_i} and R_{θ_n} are, respectively, the rotation matrices associated with rotation about the first and last axes of the first and last joints contributing to the position of the pointer-tip. The variable d_i is the distance from the origin of the body referenced coordinate system (sternum marker) to the wrist joint and sl_h is the length from the wrist to the pointer marker. p_i and p_{i+1} are, respectively, the translation vectors associated with rotation about the first and last axes of the first and last joints contributing to the direction of the pointer.

Because it is difficult to know what coordinates of the pointer-tip are planned during the course of reaching, the planned coordinates at each point throughout the reach path were estimated to be those coordinates (\underline{r}_0) that would be actualized if the mean joint configuration ($\underline{\theta}_0$) across repetitions was implemented. The matrix of partial derivatives of this geometric model relating the pointer-tip coordinates to the mean joint configuration, the Jacobian matrix [$\underline{J}(\underline{\theta}_0)$], was then determined:

$$\underline{r} - \underline{r}_0 = \underline{J}(\underline{\theta}_0) (\underline{\theta} - \underline{\theta}_0).$$

Stability of the pointer-tip's coordinates at any point along the reach across repetitions requires minimizing its deviation from the planned coordinates, i.e., $r - r_0 = 0$. This can be accomplished by either minimizing deviations of the actual joint configuration ($\underline{\theta}_i$) at each time 'I' from a hypothetical planned joint configuration ($\underline{\theta}_0$), i.e., $(\underline{\theta} - \underline{\theta}_0) = 0$, or by allowing deviations of the joint configuration $\underline{\theta}$ from $\underline{\theta}_0$ as long as those deviations maintain $r - r_0 = 0 = \underline{J}(\underline{\theta}_0) (\underline{\theta} - \underline{\theta}_0)$. The latter solution would be predicted if the CNS takes advantage of the available motor abundance (Latash et al., 2007). For the current analysis, we were most interested in the control of movement direction, or the two dimensions of 3D pointer-tip space that lie orthogonal to a vector pointing from the starting hand position to the target center. The full Jacobian for the current experiment is 3-by-10, with the three rows corresponding to the three dimensions of the global coordinate space and 10 columns representing the joint angles. Before further analysis, then, we rotated the Jacobian at each percentage of the reach into the local coordinate system with its x-axis defined by the vector pointing from starting position to the target. This 'localized' Jacobian was then reduced to include the last two rows, i.e., dimension two-by-ten, corresponding to a test of the stabilization of movement direction.

The formal test of our hypotheses were obtained by computing the null space ($\underline{\epsilon}$) of $\underline{J}(\underline{\theta}_0)$, which provides a linear estimate of the UCM, or the subspace of joint space within which variations of the joint configuration have no effect on the pointer-tip's position (Scholz & Schöner, 1999). Given that the arm's geometry changes throughout the movement, there is a different

UCM estimated at each percentage of the movement. Thus, to accomplish the analysis, the joint motions were first time-normalized to 100 frames based on the time of movement onset and the time of movement termination (see above), and the analysis was performed at each percentage of the reach.

The next step involved obtaining the joint configuration that participants' exhibited at each percentage, 'i', of the reach for a given trial 'j' (θ_{ij}), subtracting the mean joint configuration across trials at that percentage ($\theta_{ij} - \theta_{i0}$), and projecting this difference vector onto the null space, i.e., $\theta_{\parallel} = \epsilon_i * (\theta_{ij} - \theta_{i0})$ and into the orthogonal, or complementary subspace of joint space, i.e., $\theta_{\perp} = (\theta_{ij} - \theta_{i0}) - (\epsilon_i * (\theta_{ij} - \theta_{i0}))$. The variance of the projections across all trials were then computed within each subspace and normalized to the number of dimensions of that subspace. That is, control of movement direction is a 2-DOF control hypothesis. Because of motor abundance, changes in joint space that have no effect on the pointer-tip's movement direction lie within an eight dimensional subspace of joint space (i.e., 10 joint angles – 2-DOFs of pointer-tip control). Thus, the variance of projections of mean-free joint angles computed within the null space was divided by 8 (i.e., V_{UCM}), whereas the variance computed within the orthogonal subspace was divided by 2 (i.e., V_{ORT}). This normalization makes the analysis more conservative by suppressing more variance that contributes to motor abundance.

In addition, a separate analysis was performed on the individual joint contributions to V_{ORT} , i.e., variance that leads to variable pointer-tip positions, to determine if and how the joint contributions differed between the arms and the task conditions. All analyses were performed separately for acceleration and deceleration movement phases of the reach to investigate, respectively, the effects related to movement planning and those influenced by the operation of feedback processes.

2.5. Statistical Analyses

Statistical analyses were performed in SPSS 15.0 (SPSS Inc., Chicago, USA). The effects of arm (left vs. right) and target condition (UIP, UCL, UCT, CCT) on most of the spatial and temporal characteristics of the movements were evaluated using two-way repeated measures analyses of variance (RM-ANOVA). For analysis of the variable turning direction, the RM-ANOVA had factors arm (left vs. right) and target condition (UIP vs. UCL). Because a linearity difference is expected when comparing between reaches to the central target (UCT and CCT conditions) and reaches to the lateral targets after a target jump, a separate RM-ANOVA was performed investigating the effect of arm and condition on this index for conditions of reaching directed to the center target (UCT vs. CCT) and for conditions of reaching to the lateral targets in the double-step paradigm (UIP vs. UCL). Post-hoc tests with Bonferroni adjustments were used when appropriate. Three-way RM-ANOVAs also were used to examine the effects of arm (left vs. right) and target uncertainty (UCT vs. CCT) when reaching to the central target on the joint variance component (V_{UCM} vs. V_{ORT}) within each movement phase. Finally, two-way RM-ANOVAs with factors arm (left vs. right) and target uncertainty (UCT vs. CCT) were performed within each movement phase to investigate the individual joints' contribution to V_{ORT} and to investigate the effect of target uncertainty on joint angular velocities. The level of significance was set at $p < .05$.

3. Results

Fig. 2 illustrates twenty 3D pointer-tip trajectories from one representative participant reaching with the left (Fig. 2a) or right (Fig. 2b) arm. Movements to the center target under both CCT (single-step trials) and UCT (double-step trials) conditions had relatively equal straightness. Movements to UIP and UCL had relatively straight paths approximately up to the time of peak velocity, VEL_{PK} (black dots in the Fig. 2), and then more curved trajectories thereafter.

General timing (movement onset time, movement time, time to VEL_{PK} , and VEL_{PK}), and spatial (linearity index and constant and variable errors) characteristics of the left and right arm movements averaged (\pm SE) across participants are presented in Table 2 for both single-step (CCT) and double-step trials (UCT, UIP, and UCL). The times to turning of movement direction toward the new target are also presented for the UIP and UCL conditions.

3.1. Temporal Measures

MOT, or the time elapsed from the auditory signal until participants' movement initiation, did not differ between arms as revealed by a two-way RM-ANOVA (2 arms vs. 4 target conditions, $F(1,10) = 0.035$; $p = .856$). However, MOT was affected by the uncertainty of the target location ($F(3,30) = 3.548$; $p < .03$). Post-hoc tests revealed that the MOTs for UCT, UIP, and UCL conditions were approximately 65 ms longer than the CCT condition ($F(1,10) = 11.069$; $p < .01$).

A two-way RM-ANOVA (2 arms vs. 4 target conditions) indicated no significant effect of arm ($F(1,10) = 0.01$; $p = .914$) or condition ($F(3,30) = 4.19$; $p = .06$) on the time to reach VEL_{PK} . However, the movement time differed between the arms depending on the experimental condition as revealed by a significant two-way interaction ($F(3,30) = 4.7$; $p < .01$). Movement time did not differ between the arms when reaching to the center target (CCT: $F(1,10) = 1.62$; $p = .23$; UCT: $F(1,10) = 0.67$; $p = .43$). However, movement time of the left arm was longer than for the right arm for trials that required participants to redirect their reach to an ipsilaterally target-jump (UIP: $F(1,10) = 6.38$; $p < .03$). For pointer-tip VEL_{PK} , the two-way RM-ANOVA indicated a significant arm-by-condition interaction ($F(3,30) = 3.68$; $p < .025$). This difference was due to the right arm being faster than the left arm in the UIP condition ($F(1,10) = 8.67$; $p < .015$). The VEL_{PK} did not differ between the arms for the center target conditions ($F(1,10) = 2.78$; $p = .126$) nor was there an arm-by-condition interaction for the center target conditions (i.e., UCT vs. CCT; $F(1,10) = 3.2$; $p = .104$). These results from movement time and VEL_{PK} indicate that differences on other measures between CCT and UCT conditions cannot be attributed to differences in movement time or VEL_{PK} .

In general, the change in movement direction in UIP and UCL conditions occurred later than the time of VEL_{PK} , regardless of the arm used. However, a two-way RM-ANOVA revealed a significant arm-by-condition interaction for the time of turning direction ($F(2,20) = 26.77$; $p < .001$). This time was longer for UIP target compared to the UCL target only when movements were performed with the left arm ($F(1,10) = 51.627$; $p < .001$).

3.2. Spatial Measures

The two-way RM-ANOVA (2 arms vs. 2 target conditions) revealed that straighter paths were used when reaching with right arm compared to the left arm toward the center target ($F(1,10) = 5.28$; $p < .044$), regardless of the condition (i.e., UCT vs. CCT; $F(1,10) = 4.72$; $p = .055$). The condition effect was close to significant because of a slightly higher linearity index in the UCT condition. There was no significant arm-by-condition interaction ($F(1,10) = 0.202$; $p = .663$). However, for the double-step conditions in which the target actually jumped to a new location (UIP and UCL), which resulted in greater deviations from linearity, none of the effects were significant as revealed by the two-way RM-ANOVA (arm: $F(1,10) = 1.86$; $p = .203$; condition: $F(1,10) = 0.120$; $p = .736$; arm-by-condition interaction: $F(1,10) = 0.004$; $p = .954$).

A significant arm-by-condition interaction was observed for both constant ($F(3,30) = 4.56$; $p < .01$) and variable ($F(3,30) = 4.91$; $p < .01$) errors. Post-hoc tests indicated that greater constant and variable errors for UIP condition when performing with the left arm compared to other

conditions performed with either the left and right arm ($F(1,10) = 5.00$; $p < .05$ and $F(1,10) = 5.82$; $p < .04$, respectively for constant and variable errors).

Fig. 3 shows the percentage of the directional deviation for all trials and participants reaching with left (Fig. 3a) or right (Fig. 3b) arm at three time events (time of ACC_{PK} , VEL_{PK} , and DEC_{PK}). At the time of ACC_{PK} , all four conditions showed a similar trend as indicated by the undistinguished overlap of three lines representing UIP, UCL, and UCT conditions with the gray bars, which represent the distribution of directional deviations for the CCT condition. The larger range of directional deviations at the time of the ACC_{PK} is likely due to the fact that the participants' arm was secured in the initial location by a bag that was fitted around the lateral and medial aspect of the arm before the air extracted from the bag to ensure a consistent initial arm configuration and hand position for all conditions and trials. Thus, the arm was in a trough with firm sides. Although participants could exit the trough by moving the hand straight toward the target, some participants preferred to exit differently because of a tendency to scrape the arm against the sides of the air bag. Less directional deviation was observed by the time of VEL_{PK} , although the conditions were still indistinguishable. At the time of DEC_{PK} the reaches for UIP and UCL deviated substantially from a straight line. For these conditions, the directional deviations were characterized by unimodal profiles shifted to the left or right side (approximately -16.5° and $+16.5^\circ$, respectively) of the profile for center target conditions (around 0°).

Together, the characteristics of temporal and spatial measures suggested that (1) movement direction was planned to the center target for all conditions, and (2) on-line corrections of movement direction were apparent only after the time of VEL_{PK} . Based on these findings, the results of the variability analyses are presented separately for the acceleration and deceleration movement phases (see methods for more details). The results from movements directed to the same final target position (center) are the main interest in the current study and will be presented in greater detail.

3.3. Pointer-tip Variability

The results of directional variability of the pointer-tip position, averaged across participants, are presented for the UCT and CCT conditions in Figs. 4a and b, for the acceleration (left panel) and deceleration (right panel) phases, respectively.

Acceleration Phase—A two-way RM-ANOVA (2 arms vs. 2 target conditions) indicated that pointer-tip variability for the UCT was significantly higher than that for the CCT condition ($F(1,10) = 29.38$; $p < .001$) and was higher for the left arm than for the right arm ($F(1,10) = 8.52$; $p < .02$). However, a post hoc analysis indicated that there was a significant difference between the UCT and CCT conditions for the left arm ($F(1,10) = 7.042$; $p < .03$), whereas this difference was not statistically significant for the right arm ($F(1,10) = 3.82$; $p = .07$). Differences between arms were observed only for UCT condition ($F(1,10) = 6.83$; $p < .03$).

Deceleration Phase—As was the case for the acceleration phase, pointer-tip variability was significantly higher for the UCT than the CCT condition ($F(1,10) = 20.25$; $p < .001$) and for the left compared to the right arm ($F(1,10) = 7.61$; $p < .02$) during the deceleration phase as indicated by two-way RM-ANOVA (2 arms vs. 2 target conditions). The post-hoc analysis indicated that difference in pointer-tip variability between the UCT and CCT conditions also was statistically significant for the left arm ($F(1,10) = 14.11$; $p < .001$) but not for the right arm ($F(1,10) = 3.60$; $p = .09$; Fig. 4b). In addition, the difference between arms was statistically significant only for UCT condition ($F(1,10) = 8.30$; $p < .02$).

3.4. Joint Configuration Variability

Fig. 5 illustrates the components of joint configuration variability (thick lines: V_{UCM} , thin lines: V_{ORT}) related to the control of movement direction, computed using the UCM approach. Data are from one representative participant reaching toward the center target with the left (Fig. 5a) and right (Fig. 5b) arms. Overall, V_{UCM} was higher than V_{ORT} for both conditions and arms. V_{UCM} was greater for the UCT compared to the CCT condition, in particular for the left arm. The difference in V_{ORT} between the conditions varied between arms. The vertical lines in Fig. 5 demarcate the time of VEL_{PK} used as a landmark to divide the trajectory into two movement phases. The averaged across participants' components of joint configuration variance during the acceleration and deceleration phases are presented on Figs. 6a and 6b, respectively.

Acceleration Phase—Visual examination of Fig. 6a indicates that the amount of V_{UCM} was greater in UCT compared to the CCT condition. Although this difference was larger for the left arm, V_{ORT} also increased when reaching under the UCT condition with left arm. A three-way RM-ANOVA (2 arms vs. 2 target conditions vs. 2 variance components) revealed a significant condition-by-variance component interaction ($F(1,10) = 4.96; p < .05$) which corroborated our observation that the effect of target uncertainty on V_{ORT} varied between conditions. When comparing each variance component separately between the UCT and CCT conditions, we found that the difference in V_{UCM} between UCT and CCT conditions (0.0012 ± 0.0006 and 0.00044 ± 0.0001 rads^2 for left and right arm, respectively) was greater than the difference in V_{ORT} between these conditions (0.00047 ± 0.0002 and 0.00009 ± 0.00004 rads^2 for left and right arm, respectively). Although the same effect for V_{UCM} was observed for both arms, only the left arm appeared to have substantially higher V_{ORT} when reaching under target uncertainty compared to the certain target condition. However, the arm effect on this difference between UCT and CCT conditions did not reach significance for either variance component ($F(1,10) = 1.55; p = .24$ and $F(1,10) = 2.9; p = .12$ for V_{UCM} and V_{ORT} , respectively), and there was no arm-by-variance component interaction ($F(1,10) = 1.58; p = .24$ and $F(1,10) = 3.32; p = .098$ for V_{UCM} and V_{ORT} , respectively).

Each joint's variance contribution to V_{ORT} during the acceleration phase is plotted along a different axis in Fig. 7a, averaged across participants (\pm SEM). Zero variance is at the origin of the figure. Overall, the results indicate that similar joint angle motions contributed to directional variability of the pointer-tip for UCT (gray filled cones in Fig. 7) and CCT (black filled cones) conditions, although the variance of all joint motions was larger for the UCT condition. A two-way RM-ANOVA (2 arms vs. 2 target conditions) indicated that target uncertainty affected the variance contributions to V_{ORT} for all joint angle motions ($F(1,10) > 7.4; p < .02$), except elbow pronation-supination ($F(1,10) = 3.37; p = .096$). For the left arm (left panel, Fig. 7a), larger joint variance contributed to pointer-tip directional variability compared to the right arm, especially for the UCT condition. However, a main effect of arm was found only for scapula abduction-adduction ($F(1,10) = 29.05; p < .001$) and scapula upward-downward rotation ($F(1,10) = 8.89; p < .015$). A significant arm-by-condition interaction was also present for scapula abduction-adduction ($F(1,10) = 5.43; p < .05$) suggesting that larger variability of this joint's motion was present only in the UCT condition.

Deceleration Phase—The averaged across participants results for the V_{UCM} and V_{ORT} components of variance during the deceleration phase (Fig. 6b) were consistent with the individual data illustrated in Fig. 5 and the results for acceleration phase (Fig. 6a). V_{ORT} and, especially, V_{UCM} were larger for the UCT compared to CCT condition for both arms. The difference between UCT and CCT conditions was stronger for V_{UCM} compared to V_{ORT} as indicated by a significant condition-by-variance component interaction ($F(1,10) = 5.00; p < .05$). The UCT condition induced a significantly greater increase in V_{UCM} (0.0008 ± 0.0004

and $0.00075 \pm 0.0003 \text{ rads}^2$ for left and right arm, respectively) compared to the CCT condition than was the case for V_{ORT} (0.00037 ± 0.0001 and $0.00006 \pm 0.00004 \text{ rads}^2$ for left and right arm, respectively). Fig. 6b suggests that most of the difference in V_{ORT} between the UCT and CCT conditions comes from the left arm, which is confirmed by a significant arm-by-condition interaction for V_{ORT} ($F(1,10) = 6.66; p < .03$) but not for V_{UCM} ($F(1,10) = 0.12; p = .73$).

The joint angle contributions to V_{ORT} during the deceleration phase are presented in Fig. 7b. The results are relatively similar to those for the acceleration phase, with nearly all joints contributing more for the UCT compared to the CCT condition. Results from two-way RM-ANOVAs (2 arms vs. 2 target conditions) revealed significant difference between conditions for all joint motions ($F(1,10) > 5.73; p < .04$). There were also significant arm-by-condition interactions ($F(1,10) > 5.4; p < .04$) for scapula abduction-adduction and upward-downward rotation, shoulder internal-external rotation and wrist flexion-extension motions. The difference between the UCT and CCT conditions in these joint contributions to V_{ORT} was larger for the left arm.

3.5. Joint Angular Velocities

Averaged across participants joint angular velocities are presented for the UCT and CCT conditions in Table 3. The results indicate that only a few joint angular velocities differed between arms or conditions. Only the angular velocities of shoulder and wrist flexion-extension movements were affected by the target uncertainty ($F(1,10) > 5.9; p < .035$). Higher peak velocities were observed for shoulder flexion-extension motion during CCT compared to UCT condition. Wrist flexion-extension angular velocity increased slightly when reaching to the center target when there was uncertainty about the final target location. A significant arm-by-condition interaction was observed only for angular velocity of wrist abduction-adduction motion ($F(1,10) = 7.82; p < .02$). This motion was slower for the right wrist in the CCT condition compared to both the UCT condition and the left wrist's motion in either condition.

4. Discussion

The current study of right-hand dominant individuals investigated hemispheric differences in the use of motor abundance when planning reaching movements that required greater movement flexibility. We compared reaches from an identical starting joint configuration and hand position to a centrally located target under two conditions: (1) when the target location was known in advance by the participant (CCT), and (2) when there was a 66.7% probability that the target would jump to a different location (UCT). We also examined performance measures of trials requiring a change of reach direction when the target jumped (UIP and UCL). We hypothesized that the UCT condition would require more flexibility that would be reflected in planning the reach trajectories and predicted an advantage for the dominant hemisphere. No significant differences in movement onset time, the time to peak velocity, movement time, or constant and variable errors were found between the arms when reaching to the center target under either certain (CCT) or uncertain (UCT) conditions. Both arms exhibited greater use of motor abundance related to control of the reach trajectory when reaching under the uncertain compared to the certain condition. This finding provides preliminary evidence that no difference exists between the hemispheres in the ability to plan for the use of flexible combinations of joints when necessary, contrary to what we predicted. Nonetheless, although the both arms exhibited larger V_{UCM} when reaching under the uncertain condition, the left arm also had higher V_{ORT} , which was associated with increased trajectory variability. Thus, it appears that the left arm has more difficulty effectively implementing the use of additional motor abundance, leading to greater variability of the pointer-tip's movement path (see discussion below). Because performance measures such as movement time, time to peak velocity, and peak velocity itself did not differ between the arms or conditions when reaching

to the center target, the arm differences in the selective use motor abundance cannot be attributed to differences in these performance measures.

4.1. Motor abundance is a common feature of the coordination of reaching

The UCM approach provides a principled tool for examining the role of motor abundance in motor tasks (see Latash et al., 2007 for review). Previous studies using this method have provided evidence suggesting that the CNS takes advantage of motor abundance when performing reaching tasks (Reisman & Scholz, 2003; Scholz et al., 2000; Tseng & Scholz, 2005; Tseng et al., 2002). The results of the present study confirm those of an earlier study suggesting that movement planning affects the magnitude of motor abundance used (Freitas et al., 2007). This study extended the question to investigate differences between non-dominant arm/hemispheres of right-handed individuals. Our results are inconsistent with the hypothesis that a fixed final arm joint configuration typically is used to reach the same target location across repetitions (Cruse & Bruwer, 1987; Cruse, Bruwer, & Dean, 1993; Desmurget et al., 1995; Gielen, Vrijenhoek, Flash, & Neggers, 1997; Grea, Desmurget, & Prablanc, 2000; Prablanc, Desmurget, & Grea, 2003; Rosenbaum, Loukopoulos, Meulenbroek, Vaughan, & Engelbrecht, 1995), depending on the number of DOFs involved in the task (Cruse, Bruwer, & Dean, 1993). Underlying that hypothesis is the idea that the CNS plans movements, at least in part, in terms of the joint rotations that lead to an identical final posture (Haggard, Hutchinson, & Stein, 1995; Rosenbaum et al., 1995). If true, we could expect in the current experiment that values of V_{UCM} would be smaller than or equal to V_{ORT} . Instead, V_{UCM} related to stability of the reach trajectory was higher than V_{ORT} for both arms regardless of the target condition. In addition, more motor abundance was used when greater coordination flexibility likely was needed, i.e., reaching when the final target location was uncertain. These results support the conclusion of Robertson and Miall (1997) that the CNS exploits the intrinsic motor abundance of the limb to effectively control movements during an unpredictable perturbation of the target location. They are also consistent with other studies suggesting that motor abundance is typically used to control reaching movements (Haggard et al., 1995).

4.2. Constraints on the use motor abundance

In the reaching tasks studied here, transitions from one hand position to another along the movement path require an underlying transition between different UCMs. Although there are many joint combinations within a given UCM that would yield the same pointer-tip position, many of these are not the most efficient to move to the next UCM in the sequence. Thus, while, in principle, any set of joint combinations lying within the current UCM is acceptable, only a limited set of all available combinations seems to be used when the target position is well known in advance. This hypothesis has similarities with Rosenbaum and colleagues' *travel cost* of arm postures for reaching (Rosenbaum et al., 1995), although our results are at odds with the notion that fixed postures are selected for identical task constraints. Additional constraints also may limit the size of the family of solutions within the UCM that are actually realized. For example, kinematic cost factors such as minimizing jerkiness of movement (Flash & Hogan, 1985) or kinetic factors such as minimizing changes in torque or work (Biess, Liebermann, & Flash, 2007; Soechting, Buneo, Herrmann, & Flanders, 1995; Uno, Kawato, & Suzuki, 1989) have been proposed as constraints that limit the motor solutions actually utilized.

When more flexibility is required for the task, however, as when an individual knows in advance that they might have to change the direction of their ongoing reach, constraints on the range of joint combinations within the current UCM apparently can be relaxed somewhat. This was apparently the case when participants reached with either arm to the central target under the uncertain targeting conditions. One might think of this as a 'constraint-relaxation strategy'. We would emphasize that such a strategy, as well as the typical use of motor abundance,

requires that the variability of joint combinations be limited to the UCM so that there is minimal interference with task performance. This condition requires significant joint coordination, which was dependent on the arm's dominance in the current study.

4.3. Hemispheric differences exist in coordinating joint space to use motor abundance

The fact that both arms showed an increased use of motor abundance when the final target location was uncertain suggests that there were no differences between the hemispheres in planning for more movement flexibility. However, as noted above, the left arm also had consistently higher error variance (V_{ORT}), i.e., joint variance leading to inter-trial variability of the pointer-tip position at each point in the movement path, when performing the uncertain condition. Further, our analysis of the contribution of each joint motion to V_{ORT} (Fig. 7) suggested that more DOFs of the left arm contributed to this increased V_{ORT} in the UCT condition.

What might account for this arm difference? One possibility is inconsistent motor planning from trial to trial by the non-dominant hemisphere (i.e., the planning of slightly deviated target locations for each trial), which would produce both higher V_{ORT} and greater pointer-tip path variability. Because no difference between the arms was observed when the target was fixed, however, inconsistency in motor planning seems unlikely.

A more likely explanation is that the arm differences are due to differences in the ability of the hemispheres to effectively coordinate the arm DOFs. That is, according to the UCM approach a *selective* increase in motor abundance (i.e., an increase in V_{UCM} with no concomitant increase in V_{ORT}) can be accomplished only by relaxing constraints within the UCM while continuing to restrict variations of the joint configuration that would lead to unwanted variations of the pointer-tip trajectory. This requires significant coordination of joint motions, reflecting a form of decoupling of these two subspaces of joint space (Martin, 2005; Martin, Scholz, & Schöner, 2009). Our previous results from studies of dominant arm reaching suggested that the range of motor abundance used could be increased when participants needed to plan for greater movement flexibility, as when reaching to a target that could change location suddenly (Freitas et al., 2007). Thus, we believe that the difference between the arms in selectively using motor abundance results from differences in the ability of each hemisphere to achieve effective joint-space decoupling.

The poorer ability of the left, non-dominant arm to decouple joint motions to reach under the condition of target uncertainty might be attributed to limited experience with such tasks, as suggested by Tseng and colleagues (2002). Thus, these results appear to be consistent with the "dynamic dominance" hypothesis, which states that control of the dominant arm's trajectory entails more efficient and accurate coordination of muscle actions with the complex biomechanical interactions that arise between the moving segments of the limb (Sainburg & Duff, 2006). It should be noted that differences in right/left hemisphere control-processes (related to the ability to effectively decouple joint space) and greater experience with the right arm in everyday tasks are not mutually exclusive in terms of explaining the differences in this study; effective joint-space decoupling under a variety of task conditions may require experience performing under different task constraints. Future studies should examine this issue in left-handed participants. Similar findings in left-handed individuals would indicate that the selective use of motor abundance is not affected by arm dominance per se, but to a hemispheric specialization in coordinating arm movements. In fact, hemispheric specialization independent of handedness has been reported in studies using double-step paradigm (Boulinguez, Nougier et al., 2001; 2001). The conclusion of those studies was based largely on the finding of shorter reaction times for left versus right arm movements (Barthelemy & Boulinguez, 2001; Boulinguez et al., 2000; Boulinguez, Nougier et al., 2001; Carson et al., 1995; Elliot & Chua, 1996; Hodges et al., 1997). Although our participants were not required

to react as fast as possible to the auditory signal, we investigated condition differences in the time they spent between that signal and pointer-tip movement onset, which we refer to as movement onset time (MOT). No arm differences were found in this measure, which contrasts with reported reaction time results. Thus reported reaction time results likely reflect differences between the hemispheres in the ability to process information quickly.

4.4. Does the potential need for on-line corrections affect the selective use of motor abundance and pointer-tip variability differently for each arm?

The delay in initiating a change in movement direction when the target suddenly changed its location 16-ms after movement initiation was similar for both arms to that reported by other studies using the double-step paradigm (Komilis et al., 1993; Sarlegna, Blouin, Bresciani, Bourdin, Vercher, & Gauthier, 2003). This delay is likely due the fact that visual feedback takes about 200 ms to achieve on-line adjustments of the ongoing movement (van Sonderen, Denier van der Gon, & Gielen, 1988). However, the magnitude of the delay exhibited by participants participating in the current experiment was greater when reaching with the left than with the right arm, at least for the UIP condition. In addition, the left arm exhibited higher V_{ORT} and higher pointer-tip position variability along the movement path during the deceleration phase for the UCT compared to the CCT condition. The later finding was initially surprising given the presumed superiority of the right hemisphere for processing rapid, on-line visual corrections (Bagesteiro & Sainburg, 2002; Haaland & Harrington, 1989a, 1989b; Sainburg, 2002, 2005; Winstein & Pohl, 1995). Still, the right hemisphere/left arm's presumed superiority over the left hemisphere/right arm at feedback control may be indicated by the fact that although the left arm exhibited larger V_{ORT} and pointer-tip position variability during the movement deceleration phase, there were no differences in targeting error between the arms when reaching to the center target under certain or uncertain conditions. Thus, the right hemisphere was apparently able to make appropriate corrections for the left arm's larger trajectory variability during the deceleration phase of reaches to the center target in order to achieve targeting behavior comparable to that of the right arm.

Nonetheless, the longer time required for the left arm to change the direction of its movement path and the greater targeting error observed in this arm when the target actually jumped in the UIP condition suggests that the right hemisphere had greater difficulty making large on-line corrections in this condition. This finding in the condition when the target actually jumped ipsilaterally may be due to the fact that changes in the movement path towards the ipsilateral target (UIP condition) required a larger change in movement direction and subsequent modification of joint coordination, particularly with the required change from shoulder adduction to abduction, than was required when changing the pointer-tip movement path towards the contralateral target (which did not require a directional change in joint movement). Recently, Shabbott & Sainburg (2008) also observed an advantage of the dominant, right arm in making corrections to visuomotor rotations compared to the non-dominant arm if greater intersegmental coordination was required.

In addition, an advantage in controlling the effects of intersegmental limb dynamics by the dominant, right arm has been reported by several studies (Bagesteiro & Sainburg, 2002, 2003; Sainburg & Kalakanis, 2000; Shabbott & Sainburg, 2008). This asymmetry in controlling limb dynamics apparently did not affect the accuracy of the movements and was not related to the movement speed, as described by Sainburg's group. The reversal of shoulder direction required to change the pointer-tip's movement toward the ipsilateral target in the current study would require a greater adjustment of intersegmental dynamics compared to changing the pointer-tip's movement toward the contralateral target. Thus, the greater pointer-tip position variability of the left compared to the right arm observed after the target jumped ipsilaterally appears to be consistent with Sainburg's results. For those conditions, no differences in

accuracy or speed were observed. Thus, the right hemisphere apparently was able to use feedback information to effectively make on-line corrections by the time the target was reached.

4.5. Summary

The findings of the current experiment corroborate and extend our previous result suggesting that the CNS takes into account the uncertainty of movement direction during motor planning (Freitas et al., 2007), exploiting motor abundance to provide for flexible combinations of joints to be used to acquire the target while maintaining a consistent hand path. The selective structuring of joint variance primarily in directions that do not affect the value of important task parameters (i.e., greater increase in V_{UCM} compared to V_{ORT}) requires nontrivial coordination among the joint motions involved. The current results suggest that the ability of the two hemispheres to modify constraints on the joint configuration within the UCM when planning for reaches to uncertain targets appears to be equivalent. However, the right hemisphere apparently has more difficulty implementing the coordination needed to selectively increase motor abundance without also producing greater variability of left hand's movement path.

Acknowledgments

The authors would like to thank Dr. Masayoshi Kubo for assistance with technical issues related to the experiments and Andrea J. Stehman for assistance with data collection and analysis. The project described was supported by grant number NS050880 from the National Institute of Neurological Disorders and Stroke. The content is solely the responsibility of the authors and does not necessarily represent the official views of the National Institute of Neurological Disorders and Stroke or the National Institutes of Health.

References

- Bagesteiro LB, Sainburg RL. Handedness: Dominant arm advantages in control of limb dynamics. *Journal of Neurophysiology* 2002;88:2408–2421. [PubMed: 12424282]
- Bagesteiro LB, Sainburg RL. Nondominant arm advantages in load compensation during rapid elbow joint movements. *Journal of Neurophysiology* 2003;90:1503–1513. [PubMed: 12736237]
- Barthelemy S, Boultinguez P. Manual reaction time asymmetries in human subjects: the role of movement planning and attention. *Neuroscience Letters* 2001;315:41–44. [PubMed: 11711210]
- Bernstein, N. *The coordination and regulation of movements*. Oxford: Pergamon Press; 1967.
- Biess A, Liebermann DG, Flash T. A computational model for redundant human three-dimensional pointing movements: integration of independent spatial and temporal motor plans simplifies movement dynamics. *Journal of Neuroscience* 2007;27:13045–13064. [PubMed: 18045899]
- Boultinguez P, Barthelemy S, Debu B. Influence of the movement parameter to be controlled on manual RT asymmetries in right-handers. *Brain and cognition* 2000;44:653–661. [PubMed: 11104547]
- Boultinguez P, Nougier V, Velay JL. Manual asymmetries in reaching movement control. I: Study of right-handers. *Cortex* 2001;37:101–122. [PubMed: 11292156]
- Boultinguez P, Velay JL, Nougier V. Manual asymmetries in reaching movement control. II: Study of left-handers. *Cortex* 2001;37:123–138. [PubMed: 11292158]
- Carson RG, Chua R, Goodman D, Byblow WD, Elliott D. The preparation of aiming movements. *Brain and cognition* 1995;28:133–154. [PubMed: 7546669]
- Cruse H, Bruwer M. The human arm as a redundant manipulator: the control of path and joint angles. *Biological Cybernetics* 1987;57:137–144. [PubMed: 3620542]
- Cruse H, Bruwer M, Dean J. Control of three- and four-joint arm movement: strategies for a manipulator with redundant degrees of freedom. *Journal of Motor Behavior* 1993;25:131–139. [PubMed: 12581984]
- Desmurget M, Prablanc C, Rossetti Y, Arzi M, Paulignan Y, Urquizar C, et al. Postural and synergic control for three-dimensional movements of reaching and grasping. *Journal of Neurophysiology* 1995;74:905–910. [PubMed: 7472395]

- Elliot, D.; Chua, R. Manual asymmetries in goal-directed movement. In: Elliot, D.; Roy, EA., editors. *Manual Asymmetries in motor performance*. Boca Raton, Florida: CRC Press; 1996. p. 143-158.
- Elliott D, Binsted G, Heath M. The control of goal-directed limb movements: Correcting errors in the trajectory. *Human Movement Science* 1999;18:121–136.
- Elliott D, Lyons J, Chua R, Goodman D, Carson RG. The influence of target perturbation on manual aiming asymmetries in right-handers. *Cortex* 1995;31:685–697. [PubMed: 8750026]
- Flash T, Hogan N. The coordination of arm movements: An experimentally confirmed mathematical model. *Journal of Neuroscience* 1985;5:1688–1703. [PubMed: 4020415]
- Freitas SM, Scholz JP, Stehman AJ. Effect of motor planning on use of motor abundance. *Neuroscience Letters* 2007;417:66–71. [PubMed: 17331643]
- Gelfand IM, Latash ML. On the problem of adequate language in motor control. *Motor Control* 1998;2:306–313. [PubMed: 9758883]
- Georgopoulos AP, Kalaska JF, Massey JT. Spatial trajectories and reaction times of aimed movements: Effects of practice, uncertainty, and change in target location. *Journal of Neurophysiology* 1981;46:725–743. [PubMed: 7288461]
- Gielen CC, Vrijenhoek EJ, Flash T, Neggers SF. Arm position constraints during pointing and reaching in 3-D space. *Journal of Neurophysiology* 1997;78:660–673. [PubMed: 9307103]
- Grea H, Desmurget M, Prablanc C. Postural invariance in three-dimensional reaching and grasping movements. *Experimental Brain Research* 2000;134:155–162.
- Haaland KY, Harrington DL. Hemispheric control of the initial and corrective components of aiming movements. *Neuropsychologia* 1989a;27:961–969. [PubMed: 2771034]
- Haaland KY, Harrington DL. The role of the hemispheres in closed loop movements. *Brain and cognition* 1989b;9:158–180. [PubMed: 2923708]
- Haaland KY, Harrington DL, Grice JW. Effects of aging on planning and implementing arm movements. *Psychology and Aging* 1993;8:617–632. [PubMed: 8292290]
- Haaland KY, Prestopnik JL, Knight RT, Lee RR. Hemispheric asymmetries for kinematic and positional aspects of reaching. *Brain* 2004;127(Pt 5):1145–1158. [PubMed: 15033898]
- Haggard P, Hutchinson K, Stein J. Patterns of coordinated multi-joint movement. *Experimental Brain Research* 1995;107:254–266.
- Hodges NJ, Lyons J, Cockell D, Reed A, Elliott D. Hand, space and attentional asymmetries in goal-directed manual aiming. *Cortex* 1997;33:251–269. [PubMed: 9220257]
- Komilis E, Pélisson D, Prablanc C. Error processing in pointing at randomly feedback-induced double-step stimuli. *Journal of Motor Behavior* 1993;25:299–308. [PubMed: 15064196]
- Latash ML, Scholz JP, Schoner G. Toward a new theory of motor synergies. *Motor Control* 2007;11:276–308. [PubMed: 17715460]
- Liebermann DG, Biess A, Gielen CC, Flash T. Intrinsic joint kinematic planning. II: hand-path predictions based on a Listing's plane constraint. *Experimental Brain Research* 2006;171:155–173.
- Marteniuk RG, MacKenzie CL, Jeannerod M, Athènes S, Dugas C. Constraints on human arm movement trajectories. *Canadian Journal of Psychology* 1987;41:365–378. [PubMed: 3502905]
- Martin, V. A dynamical systems account of the uncontrolled manifold and motor equivalence in human pointing movements: A theoretical study. Institut für Neuroinformatik; Bochum-Germany: 2005.
- Martin V, Scholz JP, Schöner G. Using redundancy to understand how movement is generated. *Theory and experiment*. Neural Computation. 2009in press
- Oldfield RC. The assessment and analysis of handedness: the Edinburgh inventory. *Neuropsychologia* 1971;9:97–113. [PubMed: 5146491]
- Pélisson D, Prablanc C, Goodale MA, Jeannerod M. Visual control of reaching movements without vision of the limb. II. Evidence of fast unconscious processes correcting the trajectory of the hand to the final position of a double-step stimulus. *Experimental Brain Research* 1986;62:303–311.
- Prablanc C, Desmurget M, Grea H. Neural control of on-line guidance of hand reaching movements. *Progress in Brain Research* 2003;142:155–170. [PubMed: 12693260]
- Prablanc C, Martin O. Automatic control during hand reaching at undetected two-dimensional target displacements. *Journal of Neurophysiology* 1992;67:455–469. [PubMed: 1569469]

- Reisman DS, Scholz JP. Aspects of joint coordination are preserved during pointing in persons with post-stroke hemiparesis. *Brain* 2003;126(Pt 11):2510–2527. [PubMed: 12958080]
- Robertson EM, Miall RC. Multi-joint limbs permit a flexible response to unpredictable events. *Experimental Brain Research* 1997;117:148–152.
- Rosenbaum DA, Loukopoulos LD, Meulenbroek RGM, Vaughan J, Engelbrecht SE. Planning reaches by evaluating stored postures. *Psychological Review* 1995;102:28–67. [PubMed: 7878161]
- Sainburg RL. Evidence for a dynamic-dominance hypothesis of handedness. *Experimental Brain Research* 2002;142:241–258.
- Sainburg RL. Handedness: differential specializations for control of trajectory and position. *Exercise and Sport Sciences Reviews* 2005;33:206–213. [PubMed: 16239839]
- Sainburg RL, Duff SV. Does motor lateralization have implications for stroke rehabilitation? *Journal of Rehabilitation Research and Development* 2006;43:311–322. [PubMed: 17041817]
- Sainburg RL, Kalakanis D. Differences in control of limb dynamics during dominant and nondominant arm reaching. *Journal of Neurophysiology* 2000;83:2661–2675. [PubMed: 10805666]
- Sarlegna F, Blouin J, Bresciani JP, Bourdin C, Vercher JL, Gauthier GM. Target and hand position information in the online control of goal-directed arm movements. *Experimental Brain Research* 2003;151:524–535.
- Scholz JP, Schöner G. The uncontrolled manifold concept: Identifying control variables for a functional task. *Experimental Brain Research* 1999;126:289–306.
- Scholz JP, Schöner G, Latash ML. Identifying the control structure of multijoint coordination during pistol shooting. *Experimental Brain Research* 2000;135:382–404.
- Schöner G. Recent developments and problems in human movement science and their conceptual implications. *Ecological Psychology* 1995;7:291–314.
- Shabbott BA, Sainburg RL. Differentiating between two models of motor lateralization. *Journal of Neurophysiology* 2008;100:565–575. [PubMed: 18497366]
- Soderkvist I, Wedin PA. Determining the movements of the skeleton using well-configured markers. *Journal of Biomechanics* 1993;26:1473–1477. [PubMed: 8308052]
- Soechting JF. Effect of target size on spatial and temporal characteristics of a pointing movement in man. *Experimental Brain Research* 1984;54:121–132.
- Soechting JF, Buneo CA, Herrmann U, Flanders M. Moving effortlessly in three dimensions: Does Donders' law apply to arm movement? *Journal of Neuroscience* 1995;15:6271–6280. [PubMed: 7666209]
- Soechting JF, Lacquaniti F. Modification of trajectory of a pointing movement in response to a change in target location. *Journal of Neurophysiology* 1983;49:548–564. [PubMed: 6834087]
- Tseng YW, Scholz JP. The effect of workspace on the use of motor abundance. *Motor Control* 2005;9:75–100. [PubMed: 15784951]
- Tseng YW, Scholz JP, Schöner G. Goal-equivalent joint coordination in pointing: affect of vision and arm dominance. *Motor Control* 2002;6:183–207. [PubMed: 12122226]
- Uno Y, Kawato M, Suzuki R. Formation and control of optimal trajectory in human multijoint arm movement. Minimum torque-change model. *Biological Cybernetics* 1989;61:89–101. [PubMed: 2742921]
- van Soderen JF, Denier van der Gon JJ, Gielen CC. Conditions determining early modification of motor programmes in response to changes in target location. *Experimental Brain Research* 1988;71:320–328.
- Winstein CJ, Pohl PS. Effects of unilateral brain damage on the control of goal-directed hand movements. *Experimental Brain Research* 1995;105:163–174.
- Woodworth RS. The accuracy of voluntary movement. *Psychological Review* 1899;3:1–114. (Monograph Supplements)

Appendix

The Uncontrolled Manifold (UCM) method decomposes overall joint configuration variance into variance that lies in two subspaces of joint space. These two subspaces are specific to a

particular hypothesis about what task variable the CNS is trying to stabilize. One subspace, the UCM, is composed of joint combinations that do not change the current value of the task variable; variance within this subspace is referred to here as V_{UCM} . The other subspace lies orthogonal to the UCM. Variance of the joint configuration within this subspace results in variability of the task variable, which is referred to as V_{ORT} . These two components of variance are computed across trials at every point in time along the hand's path, relative to the mean joint configuration ($\underline{\theta}_0$) across trials, as follows. The goal of this analysis in the current study was to test the hypothesis that the CNS stabilizes the pointer-tip movement direction (the task variable).

A forward kinematic model links the joint configuration, $\underline{\theta}$, to the vector of the hypothesized control variable, \underline{r} , without any free parameters. The configuration of the effector system is described by a set of joint motions, $\underline{\theta}_i = (\theta_1, \dots, \theta_{10})$, where $i = 1-10$ refer to the joint motions from scapula (3 DOF), shoulder (3 DOF), elbow (2 DOF) and wrist (2 DOF) joints. Thus the number of dimensions of the "joint" configuration space is 10. The hypothesized task variable (\underline{r}) expresses a hypothesis about which DOFs are stabilized against perturbations and fluctuations. The hypothesis about stabilizing movement direction is bi-dimensional because it requires the stabilization of pointer in both y and z coordinates in a local system where the x-axis points from the initial position to the target center. Thus, our hypothesis spans a $d = 2$ -dimensional task space (or pointer-tip space) and our effector system is redundant ($n = 10 > d = 2$). The geometric model relating 3D pointer-tip movement position (\underline{r}) to the joint configuration is:

$$\begin{aligned} \underline{r} = & R_{\theta_1} * R_{\theta_2} * R_{\theta_3} * p_1 + \dots \\ & R_{\theta_1} * R_{\theta_2} * R_{\theta_3} * R_{\theta_4} * p_2 + \dots \\ & R_{\theta_1} * R_{\theta_2} * R_{\theta_3} * R_{\theta_4} * R_{\theta_5} * p_3 + \dots \\ & R_{\theta_1} * R_{\theta_2} * R_{\theta_3} * R_{\theta_4} * R_{\theta_5} * R_{\theta_6} * p_4 + \dots \\ & R_{\theta_1} * R_{\theta_2} * R_{\theta_3} * R_{\theta_4} * R_{\theta_5} * R_{\theta_6} * R_{\theta_7} * p_5 + \dots \\ & R_{\theta_1} * R_{\theta_2} * R_{\theta_3} * R_{\theta_4} * R_{\theta_5} * R_{\theta_6} * R_{\theta_7} * R_{\theta_8} * p_6 + \dots \\ & R_{\theta_1} * R_{\theta_2} * R_{\theta_3} * R_{\theta_4} * R_{\theta_5} * R_{\theta_6} * R_{\theta_7} * R_{\theta_8} * R_{\theta_9} * p_7 + \dots \\ & R_{\theta_1} * R_{\theta_2} * R_{\theta_3} * R_{\theta_4} * R_{\theta_5} * R_{\theta_6} * R_{\theta_7} * R_{\theta_8} * R_{\theta_9} * R_{\theta_{10}} * (d_i + l_h) \end{aligned} \tag{1}$$

where R_{θ_i} are the rotation matrices associated with rotation about each joint axis that contributes to the position of the pointer-tip. p_i are the translation vectors associated with the position of each joint axis from the origin of the body-referenced coordinate system. The variable d_i is the distance from the origin of the body-referenced coordinate system (sternum marker) to the wrist joint; l_h is the length from the wrist to the pointer marker.

Once computed, the joint angle trajectories were time-normalized so that different trials of movements under the same condition could be aligned. The joint configurations at each percentage of the time-normalized trajectory were analyzed across repetitions. At each percentage, the mean joint configuration across trials was computed and used to define the $d \times n$ Jacobian matrix, $\underline{J}(\underline{\theta}_0)$, of the above geometric model (1), a matrix of partial derivatives relating the pointer-tip coordinates to the mean joint configuration. Because we focus here on the 2D movement direction, we use only the last two rows of this 3×10 Jacobian matrix, the first row being related to changes in movement extent. This matrix maps small trial-to-trial changes in joint angles from the mean value ($\underline{\theta}_0$) to changes in the task variable, \underline{r} , as follows:

$$\underline{r} - \underline{r}_0 = \underline{J}(\underline{\theta}_0) (\underline{\theta} - \underline{\theta}_0), \tag{2}$$

where $\underline{\theta}_0$ is the value of the task variable corresponding to the reference configuration of joint angles, $\underline{\theta}_0$. The UCM cannot be easily determined directly, and is approximated linearly by the null-space of the $\underline{J}(\underline{\theta}_0)$, which represents combinations of joint angles that leave the task variable, here movement direction, unaffected. The basis vectors, $\underline{\varepsilon}_i$, span the null space of $\underline{J}(\underline{\theta}_0)$. We solve numerically for $\underline{\varepsilon}_i$ at each percentage of the trajectory,

$$0 = \underline{J}(\underline{\theta}_0) * \underline{\varepsilon}_i. \quad (3)$$

There are $n-d$ ($10-2$) basis vectors so that the null space has $n-d$ or eight dimensions. Deviations of the 10-dimensional joint vector from the mean joint configuration of each trial, $\underline{\theta} - \underline{\theta}_0$, were resolved into their projections onto and perpendicular to the null space:

$$\underline{\theta}_{\parallel} = \sum \underline{\varepsilon}_i * (\underline{\theta} - \underline{\theta}_0) \quad (4)$$

$$\underline{\theta}_{\perp} = (\underline{\theta} - \underline{\theta}_0) - \underline{\theta}_{\parallel} \quad (5)$$

The variance of these projections within (V_{UCM}) and perpendicular (V_{ORT}) to the UCM, normalized to the dimension of each subspace, were computed as:

$$V_{\text{UCM}} = (\sum (\underline{\theta}_{\parallel})^2 / (\text{N} - \text{trials})) * (n - d)^{-1} \quad (6)$$

$$V_{\text{ORT}} = (\sum (\underline{\theta}_{\perp})^2 / (\text{N} - \text{trials})) * (d)^{-1} \quad (7)$$

Normalization of the variances by the dimensions of the subspace compensates for differences in those dimensions, which are larger for the estimated UCM ($n-d = 8$) than for the orthogonal subspace ($d = 2$).

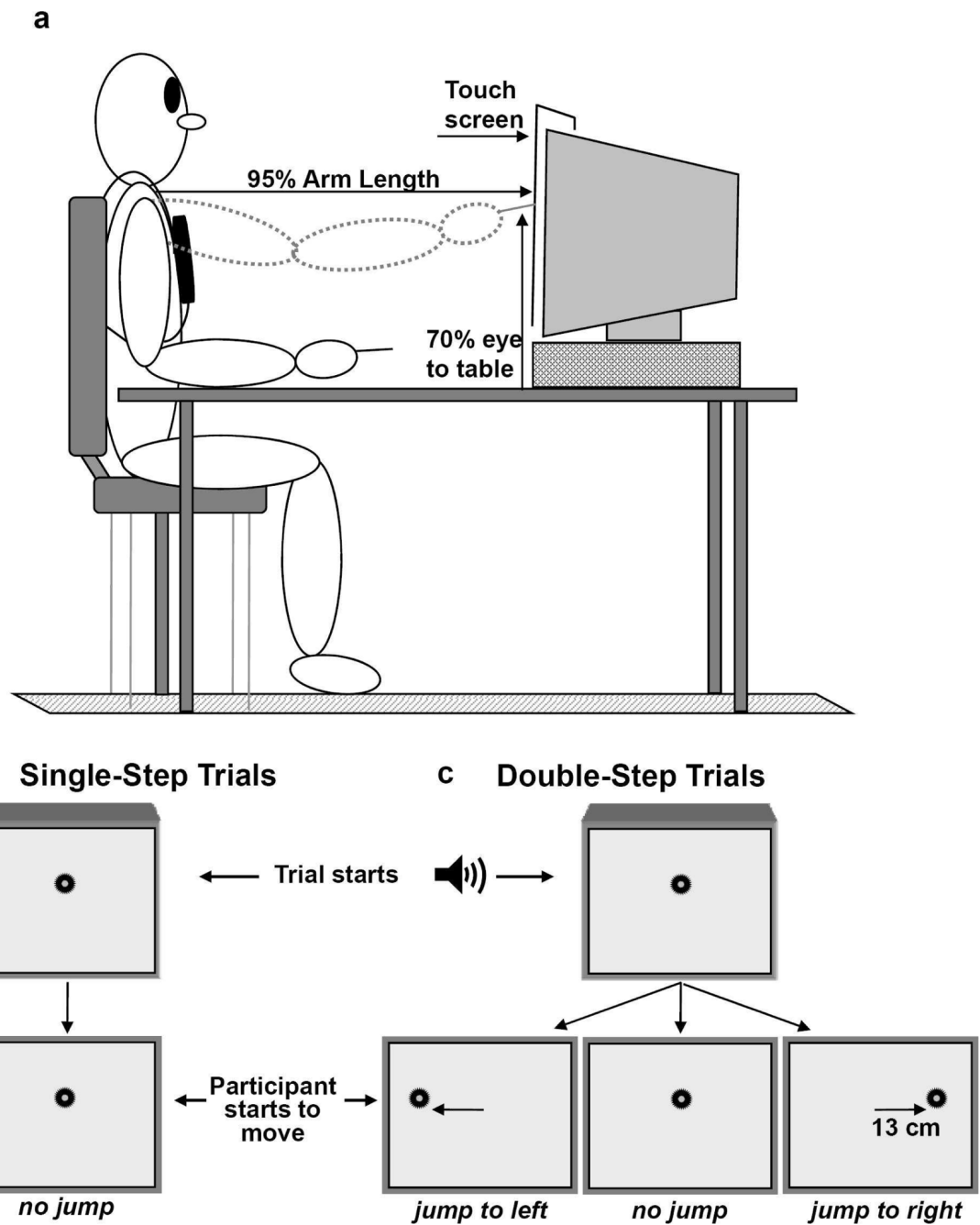


Fig. 1. Experimental Set-up (A) and target position presented at the beginning of the trial and immediately after the participants' hand starts to move for single-step (B) and double-step trials (C). For double-step trials, the target could remain at the center or jump 13 cm left or right to the central target. The presented set-up was used when the participants performed the movements with right arm. A similar set-up was used for the left arm.

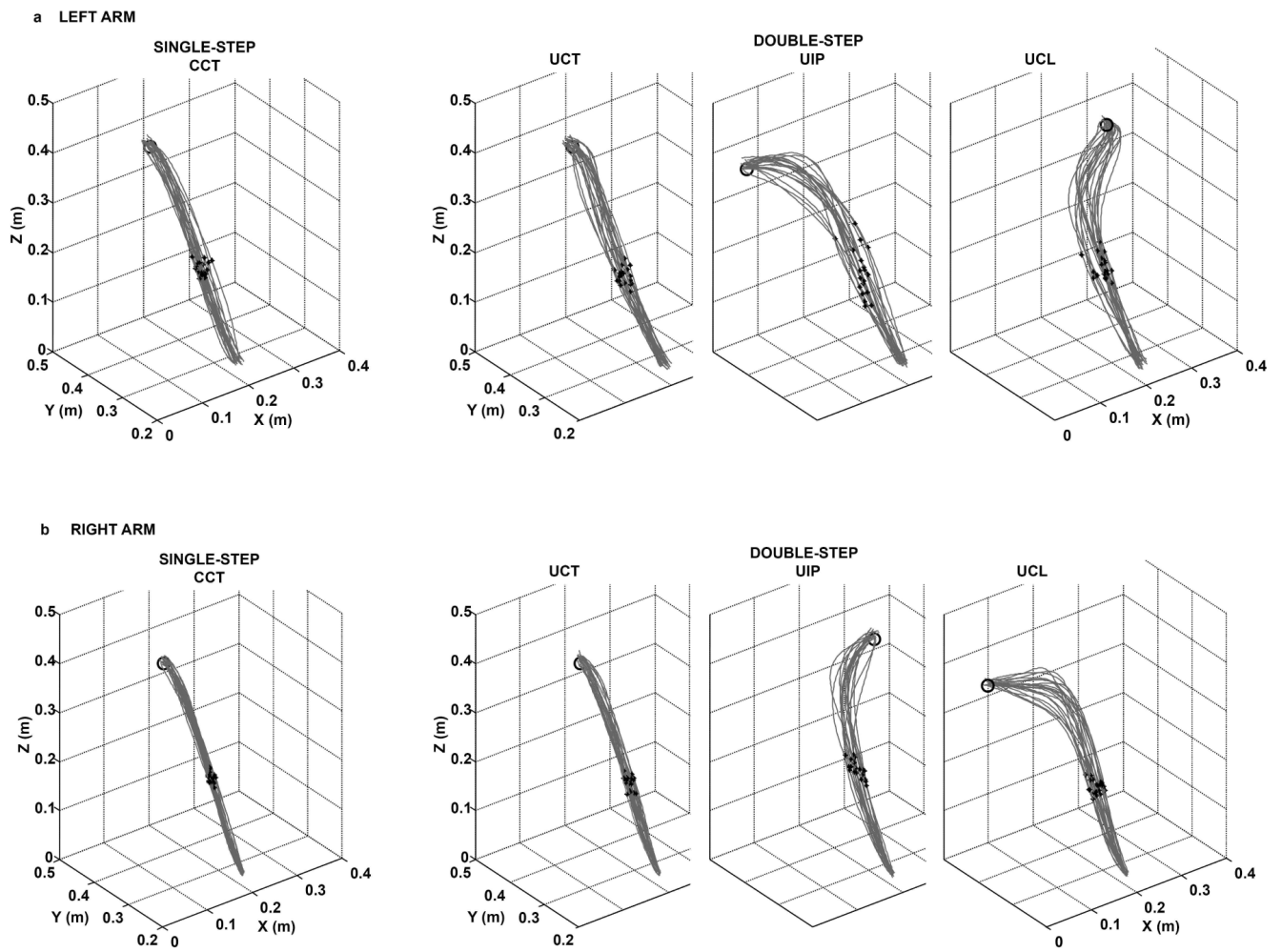


Fig. 2. Twenty 3D pointer-tip trajectories of one representative participant performing reaching movements under single-step trials to the center target (certain condition, CCT) and double-step trials to the ipsilateral target (UIP), to the center target under uncertainty target condition (UCT) and contralateral target (UCL) using (a) left arm or (b) right arm. Black circle indicates the target location for that condition and black dots indicate the time of peak velocity for each trial.

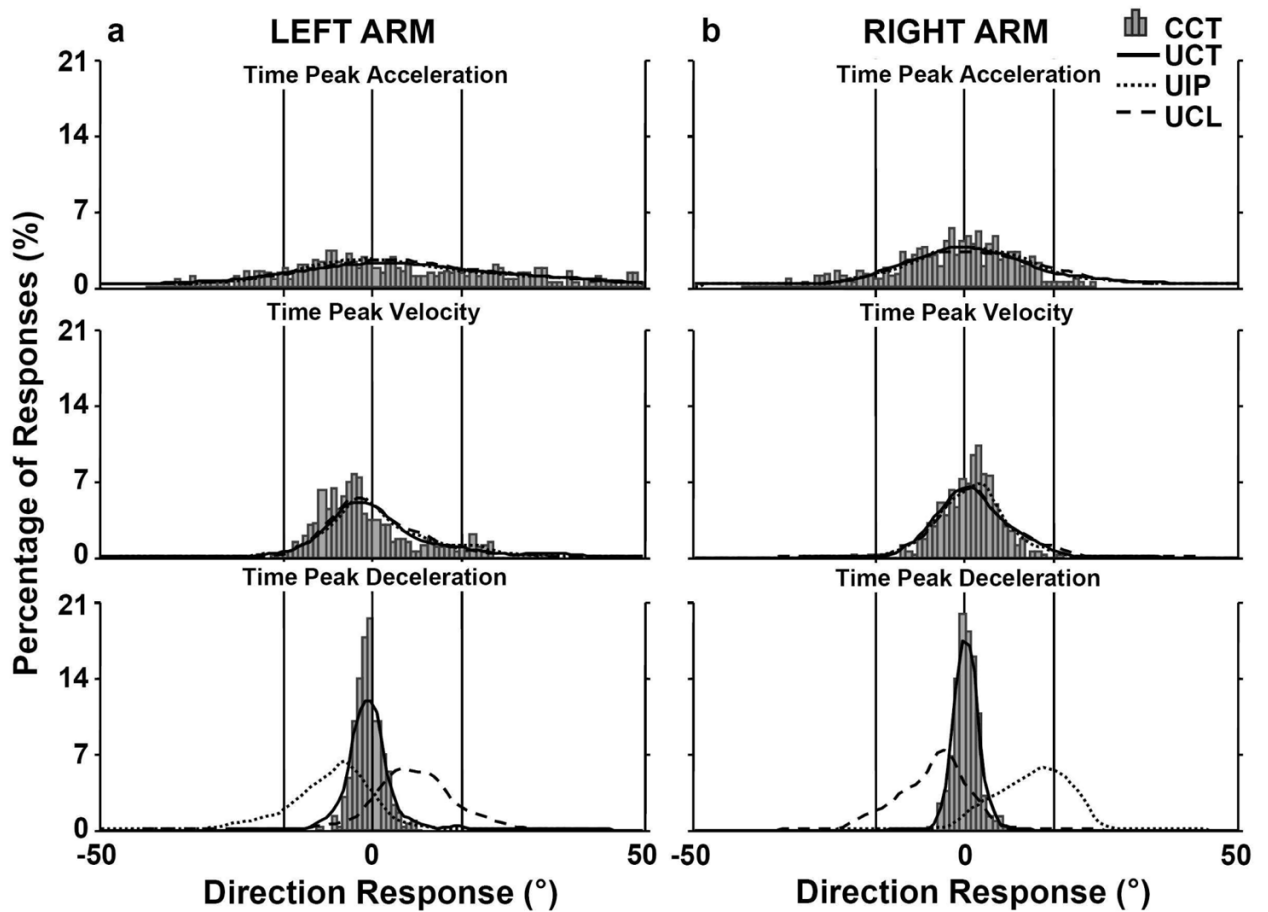


Fig. 3. Percent of directional deviations obtained at the time of Peak Acceleration, the time of Peak Velocity and the time of Peak Deceleration when the participants performed the movements using (a) left or (b) right arm for each target condition. The gray bars (histogram) correspond to the directional deviation under the CCT condition. The dotted, dashed, and solid lines correspond to ipsilateral (UIP), contralateral (UCL), and center (UCT) targets, respectively, under the uncertain target condition. The thin vertical lines represent the direction of the center target (zero degrees) and the directions of the left (right) targets relative to the center target (approximately 16.5 degrees).

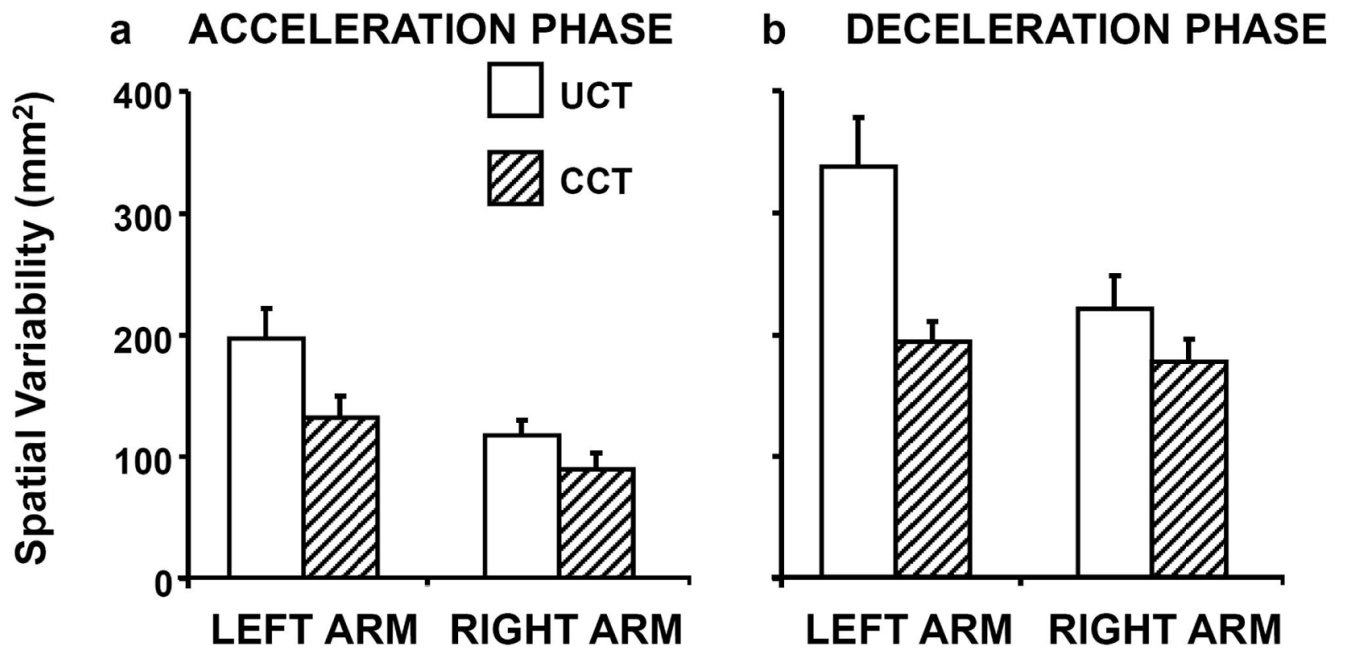


Fig. 4.

Average across-subjects pointer-tip variability related to control of movement direction, computed across the (a) Acceleration and (b) Deceleration movement phases. Bars on left (right) hand-side represent Left (Right) Arm for the uncertain (white fill) and certain (diagonal fill) conditions, when reaching to the center target. Error bars depict standard errors.

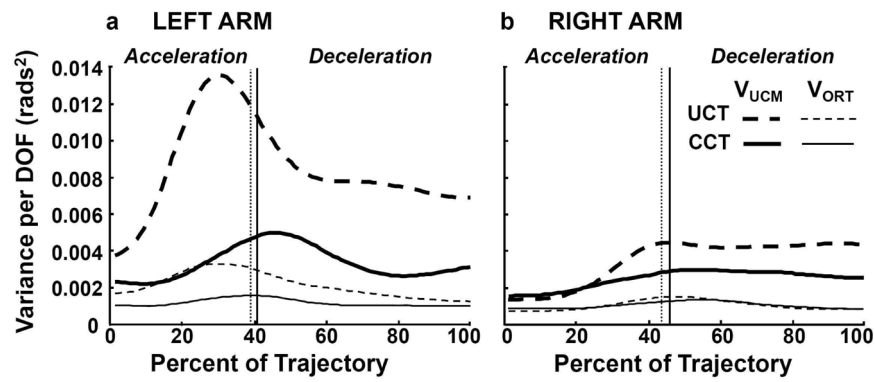


Fig. 5. Components of joint configuration variance normalized per DOF (thick lines: V_{UCM} ; thin lines: V_{ORT}) related to control of movement direction. Data are from a representative participant performing reaching to the center target when that target location was either uncertain (dashed lines) or certain (solid lines) using left (left panels) or right (right panels) arms. Vertical lines represent the time of averaged peak velocity that was used to divide the analyses in two phases (acceleration and deceleration, see methods for details).

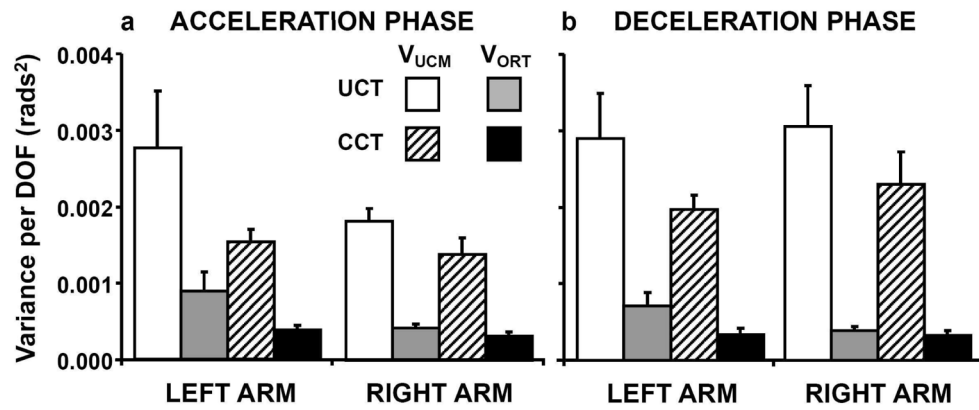


Fig. 6. Components of joint configuration variance related to control of movement direction are averaged across participants within (a) Acceleration and (b) Deceleration movement phases. Bars with white and diagonal fill represent V_{UCM} for the uncertain and certain conditions, respectively, when reaching to the center target. Gray and black filled bars show V_{ORT} for the same conditions. Error bars depict standard errors.

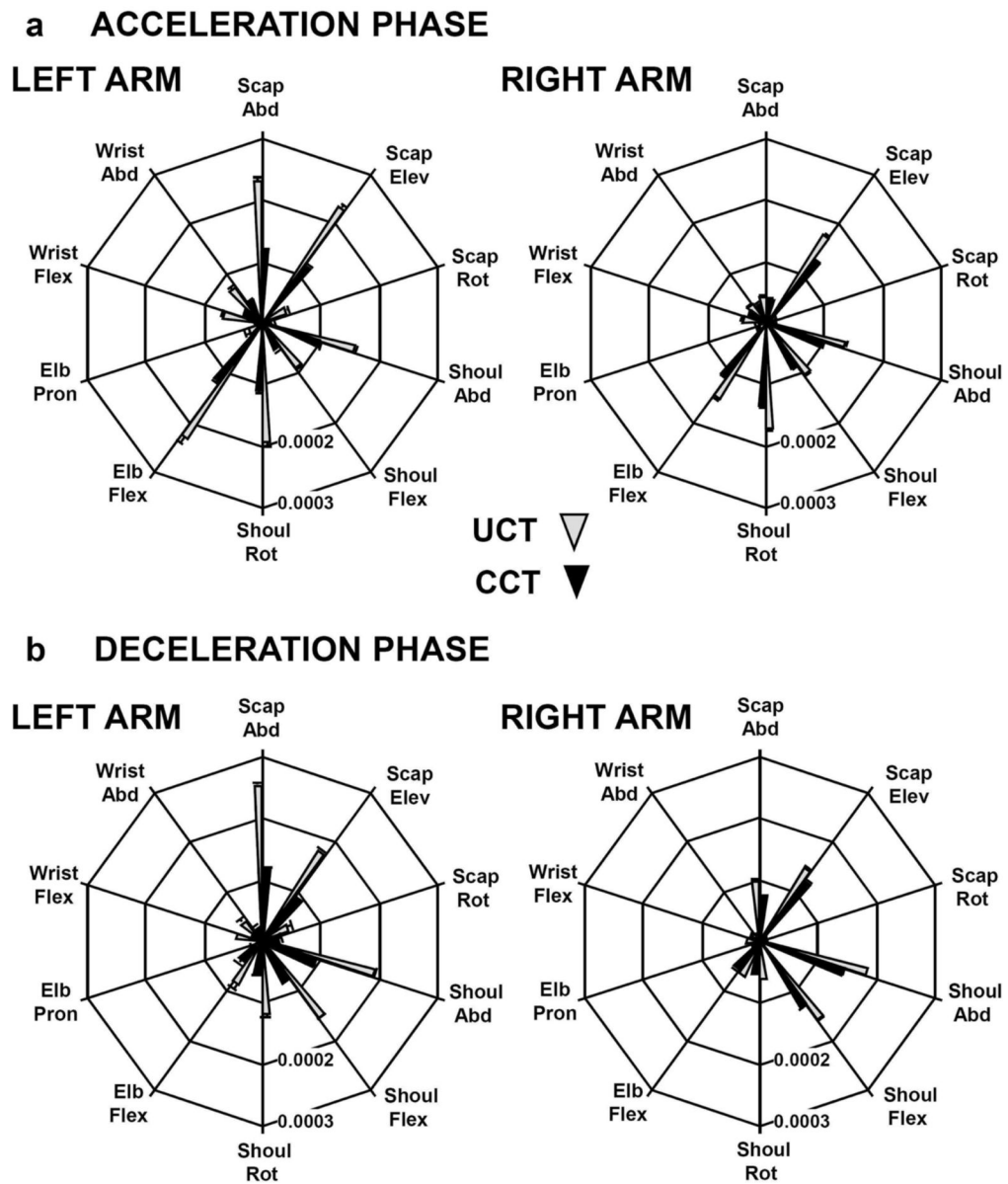


Fig. 7. Contribution of the individual joints to the joint variance component (V_{ORT}) that led to pointer-tip directional variability is depicted in polar plots. Variance, in rads^2 , is zero at the origin and increases outward to a maximum, which represents the across-subject averaged value for each condition (UCT, gray; CCT, black). Results for the acceleration movement phase are presented in A; those for the deceleration movement phase are displayed in B.

Table 1

Summary of the experimental Design. Double-Step trials were randomized across three final target locations: the target remained in the center or jumped to the right or left 16-ms following movement initiation. Asterisks represent the trials used in most analysis for comparison between arms.

Arm Target Condition	Initial Target Location		Final Target Location		Single-Step Trials	Double-Step Trials
	Left/Right	Left	Right	Center		
CCT	Center	Center	Center	Center	N = 40* (100%)	-
UCT	Center	Center	Center	Center	-	N = 40 (33%)
UIP	Center	Left	Right	Right	-	N = 40 (33%)
UCL	Center	Right	Left	Left	-	N = 40 (33%)

Table 2

General Timing and Spatial Characteristics of Arm Reaching for all four target conditions and Left and Right arms. Mean (\pm SD) movement onset time (MOT; see text for definition), movement time, time to reach the pointer Peak Velocity (VEL_{pk}) and values of pointer VEL_{pk} for all conditions, and the turning direction time in the UIP and UCL conditions are presented. Mean (\pm SD) linearity index, constant error and variable error also are presented.

Arm	Single-Step Trials (CCT)				Double-Step Trials				
	Left	Right	UCT	Left UIP	UCT	UCL	UCT	Right UIP	UCL
Temporal Measures									
MOT (ms)	390 \pm 190	377 \pm 253	463 \pm 172	470 \pm 156	444 \pm 204	454 \pm 156	444 \pm 204	454 \pm 213	461 \pm 212
Movement Time (ms)	431 \pm 53	433 \pm 41	443 \pm 57	458 \pm 58	424 \pm 45	532 \pm 53	424 \pm 45	427 \pm 45	514 \pm 47
Time to VEL _{pk} (ms)	199 \pm 20	197 \pm 22	206 \pm 17	208 \pm 15	206 \pm 21	205 \pm 12	206 \pm 21	208 \pm 20	208 \pm 21
Turning direction (ms)	-	-	-	298 \pm 28	-	230 \pm 37	-	242 \pm 20	245 \pm 43
VEL _{pk} (m/s)	1.86 \pm 0.4	1.94 \pm 0.3	1.84 \pm 0.3	1.83 \pm 0.3	1.82 \pm 0.3	1.82 \pm 0.3	2 \pm 0.3	2.03 \pm 0.4	1.99 \pm 0.4
Spatial Measures									
Linearity Index	1.07 \pm 0.04	1.04 \pm 0.03	1.09 \pm 0.06	1.15 \pm 0.08	1.05 \pm 0.03	1.14 \pm 0.06	1.05 \pm 0.03	1.13 \pm 0.06	1.13 \pm 0.05
Constant Error (cm)	1.2 \pm 0.3	1.0 \pm 0.3	1.3 \pm 0.3	3.5 \pm 1.8	1.2 \pm 0.3	1.2 \pm 0.3	1.2 \pm 0.3	2.4 \pm 1.2	1.1 \pm 0.4
Variable Error (cm)	0.9 \pm 0.1	0.8 \pm 0.2	1.0 \pm 0.2	2.2 \pm 0.7	0.9 \pm 0.3	1.0 \pm 0.2	0.9 \pm 0.3	1.8 \pm 0.7	1.0 \pm 0.4

Mean (\pm SD) peak velocity of all joint angle motions for CCT and UCT conditions. Data are presented in radians per second (rad/s). Statistically significant main effects of target condition and interaction arm-by-target condition are indicated by * and **, respectively.

Table 3

Arm Joints	DOF	Single-Step Trials (CCT)		Double-Step Trials (UCT)	
		Left	Right	Left	Right
Scapula	Abd-Adduction	1.53 \pm 0.64	1.37 \pm 0.40	1.52 \pm 0.63	1.43 \pm 0.34
	Elevation	0.85 \pm 0.36	0.62 \pm 0.41	0.80 \pm 0.38	0.63 \pm 0.39
	Rotation	0.31 \pm 0.35	0.24 \pm 0.18	0.29 \pm 0.34	0.22 \pm 0.19
Shoulder	Abd-Adduction	2.80 \pm 1.61	3.95 \pm 1.37	2.78 \pm 1.66	3.90 \pm 1.54
	Flexion-Ext*	2.59 \pm 1.33	3.30 \pm 0.82	2.45 \pm 1.21	3.14 \pm 0.81
	Rotation	2.65 \pm 0.79	3.18 \pm 1.36	2.75 \pm 0.86	3.25 \pm 1.26
	Flexion-Ext	4.14 \pm 1.64	4.40 \pm 0.97	3.89 \pm 1.50	4.31 \pm 0.92
Elbow	Pron-Supination	1.65 \pm 1.04	1.27 \pm 0.64	1.60 \pm 1.02	1.32 \pm 0.61
	Flexion-Ext*	0.92 \pm 0.71	0.79 \pm 0.43	1.06 \pm 0.63	1.05 \pm 0.48
	Abd-Adduction* **	1.05 \pm 1.46	0.30 \pm 0.56	1.27 \pm 1.38	0.95 \pm 0.81